MATHEMATICAL MODEL AND NUMERICAL SIMULATIONS FOR CONTROL THE CONNECTING-ROD CRANKSHAFT ENGINE WITH COMPRESSED AIR

Alexandre de Castro Alves
UTFPR
alexandrealves@utfpr.edu.br

Angelo Marcelo Tusset
UTFPR
tusset@utfpr.edu.br

Vinícius Piccirillo
UTFPR
piccirillo@utfpr.edu.br

José Manoel Balthazar
UNESP-ITA
jmbaltha@gmail.com

Atila Madureira Bueno
UNESP
atila@sorocaba.unesp.br

Abstract. *Numerical results of the nonlinear dynamics with compressed air engine and a single cylinder with three degrees of freedom as a triple pendulum simplified to a degree of freedom in the application of angular control on the output crankshaft were obtained. The mathematical model can be obtained through dynamic analysis of several rigid bodies with unilateral restrictions on the pneumatic cylinder and connecting-rod crankshaft. However, to simplify the implementation of the control of the angular position of the output shaft depending on the linear position of the cylinder, the nonlinear model was linearized. Numerical results show that it is possible to obtain parameters for the control of the nonlinear dynamic model of the single cylinder engine from the linearized model and analyze the parametric error.*

Keywords: *multibody system, connecting-rod crankshaft, nonlinear system, nonlinear dynamics*

1. INTRODUCTION

The connecting-rod crankshaft mechanism is one of the most important mechanisms in modern technology and is one of the fundamental elements to convert the translational into a rotating motion. There are many connecting-rod crankshaft mechanism applied to power motion control, such as combustion, hydraulic and pneumatic. However, the compressed air engine will not only be more efficient sometimes but may be the only device that can be used in some industries such as in the mining industry. A study by Pandian *et al.*, (1997) demonstrates that the major advantages of pneumatic actuators are their high payload-to-weight and payload-to-volume ratios, and their high speed and force capabilities. In this paper, we proposed the control of the nonlinear dynamic of a compressed air motor with one degree of freedom in the application of angular control on the output crankshaft.

There are various reports in the literature regarding connecting-rod crankshaft with input motion by crankshaft with self-tuning control method to position the slider cylinder (Liniecki, 1970; Wauer and Bührle, 1997; Karkoub, 2000; Lin, et al., 2001; Kao et al., 2006; Ha et al., 2006; Chuang, et al., 2006; Chuang, 2007; Fung et al., 2009; Ahmad et al., 2011).

However, there are few reports on this connecting-rod crankshaft with motion input by sliding cylinder with compressed air or per combustion. Benhammouda and Vazquez-Leal (2015) solved multibody problems for the nonlinear connecting-rod crankshaft applying three differential-algebraic equations system. Awrejcewicz and Kudra (2003) present a mono-cylinder combustion connecting-rod crankshaft engine modeled as with triple physical pendulum with barriers and six piston movements from one side of the cylinder to the other. Komaita and Furuta (2008) present a control design for the velocity control of the slider-crank mechanism based on energy control.

This study presents modeling and control of a connecting rod-crank mechanism with sliding cylinder, similar to the modeling presented by Boyle et al (2003). However to implement the control Linear quadratic regulator (LQR) the non-linear system is linearized as a simplified linear function, similar to that shown by Kao *et al.* (2006) with control applied in a transfer function.

2. DYNAMIC MODEL

For modeling the nonlinear dynamic behavior of the connecting-rod crankshaft mechanism is applied the classical mechanics formulation by Lagrange's method by combining energy conservation, and linear momentum. The Lagrangian formulation ($\mathcal{L}$) considers the difference between the kinetic energy (T) and potential energy (V).

$$\mathcal{L} = T - V \tag{1}$$

To formulate T, the mechanism motion is analyzed both in translation and in rotation on the basis of their inertia. However, the Center of Gravity (CG) of each link translates the motion along the way, depending on the restriction connections. In other words, the mechanism moves each connection rotation or translation around its CG. The potential energy V has gravitational potential and its CG determines the elastic potential.

In this paper, the nonlinear dynamic system is a connecting-rod crankshaft mechanism with rigid links. This mechanism acts as a motor with compressed air to move through the entrance for the gas force (*Fg*) as a function of air pressure. In this connecting-rod crankshaft mechanism, the air pressure generates the force (*Fg*) in a mono-cylinder link 4 (*l4*). This link takes a position change via the third link (*l3*), which turns its movement to rotate the crankshaft output of the link 2 (*l2*) as shown in Fig. 1.

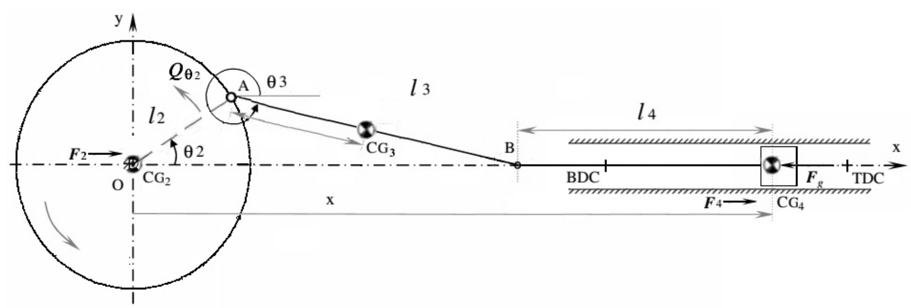

Figure 1. Connecting-rod crankshaft engine with compressed air

In terms of coordinates the system behaves like a triple pendulum with three degrees of freedom considering small displacements to the cylinder (Awrejcewicz and Kudra, 2003). However, to simplify this study the mechanism will be considered with one degree of freedom with the entry into x and the output dependent on this position θ_2.

$$x_4 = l_2\left[\cos\theta_2 - (1/2)(l_2/l_3)\sin^2\theta_2\right] + l_3 + l_4 \tag{2}$$

In this connecting-rod crankshaft mechanism, the cylinder has the highest displacement when it is in the Top Dead Center (TDC) and moves to the Bottom Dead Centre (BDC). From the TDC for BDC this mechanism oscillates from 0 to - π or rotates from 0 to - 2π. However for use in systems for mining processes in which the system will be utilized, this cylinder course will be limited to -π / 4 and - 3π / 4 as the reference of the angular movement to the exit.

2.1 The pseudo-rigid-body model

The Boyle et al. (2003) pseudo-rigid-body model (PRBM) has geometry similar to the connecting-rod crankshaft model of this study. The PRBM applies force (*Fb*) in the slider link 6 which generates a deformation of the link 3 and which transmits force for to the link 2 where there is another free end for its rotation (Fig. 2). In the transformation of the flexible link 3 to rigid the length l is replaced according to the characteristic relation of the pseudo-rigid connection (link 3 and link 6).

In the PRBM, the flexible link is represented by the combination of the hard link 3 with a torsion spring with constant k equivalent to potential energy union of links 3 and 6. This constant equivalent (k) relates the characteristic of pseudo-rigid connection (γ), the spring stiffness coefficient twist (K_Θ), the modulus of elasticity (E) of the flexible segment (l) and the flexible segment moment of inertia (I) as shown:

$$k = \frac{\gamma K_\theta E I}{l} = \frac{r_3}{l}\frac{K_\theta E I}{l} = \frac{r_3 K_\theta E I}{l^2} \tag{3}$$

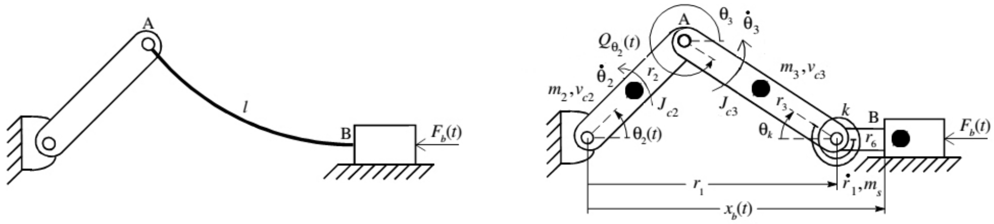

Figure 2. PRBM Model (adapted from Boyle *et al*. 2003)

In the PRBM the total mass m_s was considered as the sum of rod 6 and the mass of the slide as a rigid body which cannot rotate. With the masses, geometry and material constants set, the Lagrangian can be expressed to one degree of freedom only in terms of the generalized coordinate (θ_2), its derivative ($\dot{\theta}_2$) with respect to time and the generalized forces and their momentum with respect to time (t).

$$\frac{d}{dt}\left(\frac{\partial \mathcal{L}}{\partial \dot{\theta}_2}\right) - \frac{\partial \mathcal{L}}{\partial \theta_2} = Q_{\theta 2} \tag{4}$$

The Lagrangian function is given by

$$\mathcal{L} = T - V = \frac{1}{2} m_2\, v_{c2}^2 + \frac{1}{2} m_3\, v_{c3}^2 + \frac{1}{2} m_s\, \dot{r}_1^2 + \frac{1}{2} J_{c2}\, \dot{\theta}_2^2 + \frac{1}{2} J_{c3}\, \dot{\theta}_3^2 - \frac{1}{2} k\, \theta_k^2 \tag{5}$$

where (θ_2) is our generalized coordinate, and

vc_i = kinetic speed of the link i;
Jc_i = moment of inertia of the link i;
θ_i =angular position of link i;
k = constant deformation of material equivalent to the PRBM.

Using the Eq. (4) we can have the equation of motion

$$\begin{aligned}
&\left(\begin{aligned} &m_3\left(\frac{r_2^5\sin^3\theta_2\cos^2\theta_2}{2\,\alpha^{3/2}} + \frac{r_2^4 r_3^2\sin\theta_2\cos^3\theta_2}{3\,\alpha^2} - \frac{r_2^3\sin^3\theta_2}{2\,\alpha^{1/2}} + \frac{r_2^3\sin\theta_2\cos^2\theta_2}{\alpha^{1/2}} - \frac{r_2^2 r_3^2\sin\theta_2\cos\theta_2}{3\,\alpha} + r_2^2\sin\theta_2\cos\theta_2\right) + \\ &m_s\left(\frac{r_2^6\sin^3\theta_2\cos^3\theta_2}{\alpha^2} + \frac{r_2^5\sin^3\theta_2\cos^2\theta_2}{\alpha^{3/2}} - \frac{r_2^4\sin^3\theta_2\cos\theta_2}{\alpha} + \frac{r_2^4\sin\theta_2\cos^3\theta_2}{\alpha} + 2\frac{r_2^3\sin\theta_2\cos^2\theta_2}{\alpha^{1/2}} - \frac{r_2^3\sin^3\theta_2}{\alpha^{1/2}} + r_2^2\sin\theta_2\cos^2\theta_2\right)\end{aligned}\right)\dot{\theta}_2^2 \\
&+ \left(m_2\frac{r_2^2}{3} + m_3\left(\frac{r_2^3\sin^2\theta_2\cos\theta_2}{\alpha^{1/2}} + \frac{r_2^2 r_3^2\cos^2\theta_2}{3\,\alpha^{1/2}} + r_2^2 - r_2^2\cos^2\theta_2\right) + m_s\left(\frac{r_2^4\sin^2\theta_2\cos^2\theta_2}{\alpha} + 2\frac{r_2^3\sin^2\theta_2\cos\theta_2}{\alpha^{1/2}} + \frac{r_2^2\sin^2\theta_2}{\alpha}\right)\right)\ddot{\theta}_2 \\
&+ \frac{k\ arc\ \sin\left[(r_2/r_3)\sin\theta_2\right] r_2\cos\theta_2}{\alpha^{1/2}} - Q_{\theta 2} = 0
\end{aligned} \tag{6}$$

where

$$\alpha = r_3^2 - r_2^2\, sin^2\theta_2 \tag{7}$$

$$Q_{\theta 2} = -\tau_{Fb} + \tau_f + \tau \tag{8}$$

The generalized forces provide the momentum acting on the sliding cylinder τ_{Fb} and the forces resistant to the friction τ_f and the term τ just to offset the torques not modeled.

2.2 Nonlinear rigid-multibody model

Figure 3 shows the desired angular positions ranging from - π / 4 to - 3π / 4 depending on the geometry and application of compressed air force. These positions are a function of the variation of air pressure, that is, the pressure and input power are controlled by pneumatics valves and which is not part of this study.

These positions were defined as the course required for a screening mechanism to be used in the mining industry. This type of industry needs pneumatic energy and easy motion of their equipment, for greater flexibility and less risk of short circuit in comparison to electric motors, which can cause explosions in the mines.

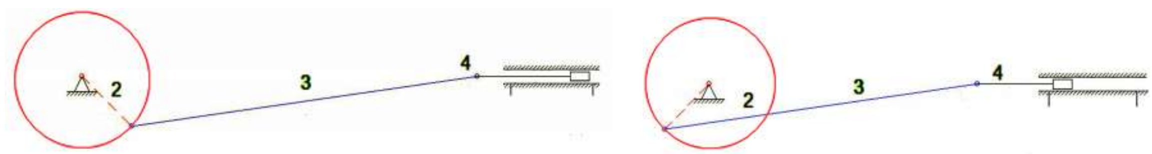

Figure 3. Positions of the control mechanism

The equation of motion with the new geometry as a function of the coordinates and generalized forces becomes

$$\left(\begin{array}{l} m_3\left(\frac{l_2^5\sin^3\theta_2\cos^2\theta_2}{2\,\beta^{3/2}}+\frac{l_2^4 l_3^2\sin\theta_2\cos^3\theta_2}{3\,\beta^2}-\frac{l_2^3\sin^3\theta_2}{2\,\beta^{1/2}}+\frac{l_2^3\sin\theta_2\cos^2\theta_2}{\beta^{1/2}}-\frac{l_2^2 l_3^2\sin\theta_2\cos\theta_2}{3\,\beta}+l_2^2\sin\theta_2\cos\theta_2\right)+ \\ m_4\left(\frac{l_2^6\sin^3\theta_2\cos^3\theta_2}{\beta^2}+\frac{l_2^5\sin^3\theta_2\cos^2\theta_2}{\beta^{3/2}}-\frac{l_2^4\sin^3\theta_2\cos\theta_2}{\beta}+\frac{l_2^4\sin\theta_2\cos^3\theta_2}{\beta}+2\frac{l_2^3\sin\theta_2\cos^2\theta_2}{\beta^{1/2}}-\frac{l_2^3\sin^3\theta_2}{\beta^{1/2}}+l_2^2\sin\theta_2\cos^2\theta_2\right) \end{array}\right)\dot{\theta}_2^2$$
$$+\left(m_2\left(\frac{l_2^2}{2}\right)+m_3\left(\frac{l_2^3\sin^2\theta_2\cos\theta_2}{\beta^{1/2}}+\frac{l_2^2 l_3^2\cos^2\theta_2}{3\,\beta^{1/2}}+l_2^2-l_2^2\cos^2\theta_2\right)+m_4\left(\frac{l_2^4\sin^2\theta_2\cos^2\theta_2}{\beta}+2\frac{l_2^3\sin^2\theta_2\cos\theta_2}{\beta^{1/2}}+\frac{l_2^2\sin^2\theta_2}{\beta}\right)\right)\ddot{\theta}_2 \quad (9)$$
$$-\,m_3\left(\frac{g l_2 cos\theta_2}{2}\right)+b_2\dot{\theta}_2-\tau_U=0$$

where

$$\beta = l_3^2 - l_2^2\, sin^2\theta_2 \tag{10}$$

$$\tau_{U=}-\tau_{Fg}+\tau_{F4} \tag{11}$$

The term τ_U represents the motion input resultant. The τ_{F4} represents the viscous friction of the sliding function of translational speed. The term b represents the viscous coefficient for the rotary motion.

2.3 Numerical simulations whitout control

The equations of motion in State-Space form are given by the system equations (12).

$$\dot{x}_1 = x_2$$
$$\dot{x}_2=\left(\frac{1}{\left(m_2\left(\frac{l_2^2}{2}\right)+m_3\left(\frac{l_2^3\sin^2 x_1\cos x_1}{\beta^{1/2}}+\frac{l_2^2 l_3^2\cos^2 x_1}{3\,\beta^{1/2}}+l_2^2-l_2^2\cos^2 x_1\right)+m_4\left(\frac{l_2^4\sin^2 x_1\cos^2 x_1}{\beta}+2\frac{l_2^3\sin^2 x_1\cos x_1}{\beta^{1/2}}+\frac{l_2^2\sin^2 x_1}{\beta}\right)\right)}\right)$$
$$\left(-\left(\begin{array}{l} m_3\left(\frac{l_2^5\sin^3 x_1\cos^2 x_1}{2\,\beta^{3/2}}+\frac{l_2^4 l_3^2\sin x_1\cos^3 x_1}{3\,\beta^2}-\frac{l_2^3\sin^3 x_1}{2\,\beta^{1/2}}+\frac{l_2^3\sin x_1\cos^2 x_1}{\beta^{1/2}}-\frac{l_2^2 l_3^2\sin x_1\cos x_1}{3\,\beta}+l_2^2\sin x_1\cos x_1\right) \\ +m_4\left(\begin{array}{l}\frac{l_2^6\sin^3 x_1\cos^3 x_1}{\beta^2}+\frac{l_2^5\sin^3 x_1\cos^2 x_1}{\beta^{3/2}}-\frac{l_2^4\sin^3 x_1\cos x_1}{\beta}+\frac{l_2^4\sin x_1\cos^3 x_1}{\beta} \\ +2\frac{l_2^3\sin x_1\cos^2 x_1}{\beta^{1/2}}-\frac{l_2^3\sin^3 x_1}{\beta^{1/2}}+l_2^2\sin x_1\cos^2 x_1\end{array}\right)\end{array}\right)x_2^2 \\ +\,m_3\left(\frac{g l_2 cos x_1}{2}\right)-b x_2+\,\tau_U\right) \tag{12}$$

The parameters used in the numerical simulations are presented in Table 1.

Table 1. Parameters of the connecting-rod crankshaft

Parameters	Value	Unit (S.I.)
θ_2	– π/4 a – 3π/4	rad
x_4	0,056	m
m_2	1,0	kg
m_3	0,5	kg
m_4	0,5	kg
l_2	0,04	m
l_3	0,2	m
g	9,8	m/s²
b	0,001	N.m/s

For the virtual work but without the use of control we will use F_g as excitation for air compressed in the pneumatic cylinder as shown in the equation.

$$F_g = 1\ (\ (\ 0{,}056/2\ )\ \text{square}\ (\ 2\ t\ ) + 0{,}056/2\ ) \tag{13}$$

Figure 4 shows the uncontrolled nonlinear system (12) by applying equation (13) and the parameters of Table 1. Where $\theta_2 = x_1 = -\dfrac{\pi}{2}$ for the condition initial.

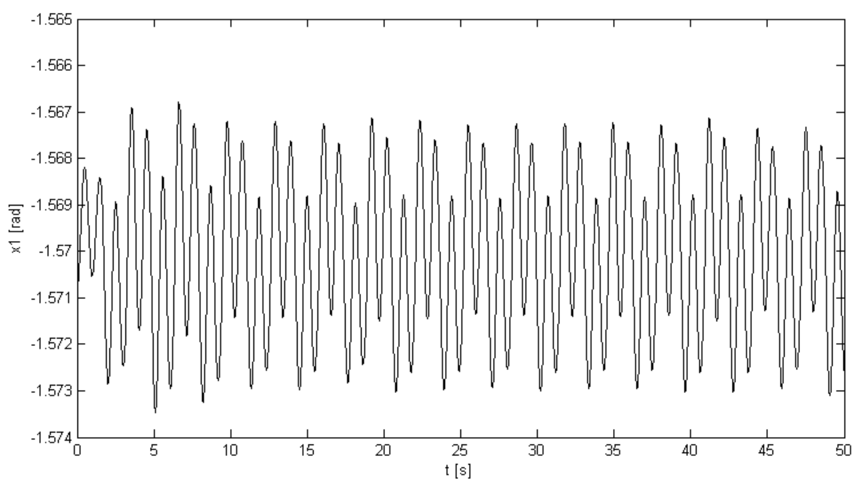

Figure 4. Nonlinear system (12)

Figure 4 shows that the oscillations are below expectations of - π / 4 to - 3π / 4 (Fig. 3). Thus, becomes necessary the control of the nonlinear dynamic system.

3. CONTROL DESIGN USING LQR TECHNIQUE

Considering the introduction of control in the equation of motion (12) the result can be obtained as show (Pedroso, *et al.,* 2013; Tusset, *et al*., 2013):

$$\dot{\mathbf{X}} = \mathbf{AX} + \mathbf{BU} \tag{14}$$

where: $\mathbf{X} = [x \quad y]^T$, $\mathbf{A}_{nxn}$ is the state matrix, $\mathbf{B}_{nxm}$ constant matrix, $\mathbf{U}$ is the control signal, which increases the system power according to the increase of air pressure to the control point (or desired orbit) and can be obtained from:

$$\mathbf{U} = -\mathbf{R}^{-1}\mathbf{B}^{\mathbf{T}}\mathbf{PZ} \tag{15}$$

where: $\mathbf{Z}=\begin{bmatrix} x-x^* \\ y-y^* \end{bmatrix}$, assuming that $\mathbf{P}_{(nxn)}$ is the solution for the Riccati equation given by:

$$\mathbf{A^T P + PA - PBR^{-1}B^T P + Q = 0} \tag{16}$$

where: $\mathbf{Q}_{nxn}$ and $\mathbf{R}_{nxm}$ are positive semi-definite matrices.

The choice of matrix must be made appropriately, according to the control system of interest. An important factor for this choice is not violating the controllability of the system. That is, the controllability matrix: $\left[\mathbf{B} \quad \mathbf{AB} \quad \ldots \quad \mathbf{A^{(n-1)}B}\right]$ must have full rank.

According to Tusset and Rafikov (2004) the matrix can be obtained from the linearization of the equilibrium points of the nonlinear system (12). Calculating the Jacobian matrix, the system (12) applied in stable equilibrium point $P=(-\frac{\pi}{2},0)$, becomes:

$$\mathbf{A}=\begin{bmatrix} 0 & 1 \\ -40.8333 & -0.4167 \end{bmatrix} \tag{17}$$

with $\mathbf{A}$ being controllable

Therefore, in the nonliner system the equilibrium point will be stable locus**.** Considering the matrix $\mathbf{A}$, the linearized control system with $\mathbf{U}$ and excitation force (13) is given by:

$$\begin{aligned} \dot{x}_1 &= x_2 \\ \dot{x}_2 &= -40.8333x_1 - 0.4167x_2 + U \end{aligned} \tag{18}$$

Considering the matrix $\mathbf{A}$ and the other matrices:

$$\mathbf{B}=\begin{bmatrix} 0 \\ 1 \end{bmatrix} \tag{19}$$

$$\mathbf{Q}=\begin{bmatrix} 10^4 & 0 \\ 0 & 10^4 \end{bmatrix} \tag{20}$$

and $\mathbf{R}=10^{-3}$ (21)

Replacing the matrices $\mathbf{A}$, $\mathbf{B}$, $\mathbf{Q}$ and $\mathbf{R}$ on the Riccati equation (16) can provide $\mathbf{P}$:

$$\mathbf{P}=\begin{bmatrix} 1000{,}9381 & 3.121 \\ 3.121 & 3.1628 \end{bmatrix} \tag{22}$$

Replacing the matrix (19) in equation (15), can provide the control signal:

$$\mathbf{U}=-3121.7079(\mathrm{x}_1-\mathrm{x}_1^*)-3162.8480(\mathrm{x}_2-\mathrm{x}_2^*) \tag{23}$$

Figure 5 shows the system behavior (18) for the excitation (13) and (23) is the desired states provided for Fig. 3, given by: $x_1^*=\frac{\pi}{4}\sin(2t)-\frac{\pi}{2}$, $x_2^*=\frac{\pi}{2}\cos(2t)$. However, for the better visualization of control for the system changed the initial condition for the position = 0.

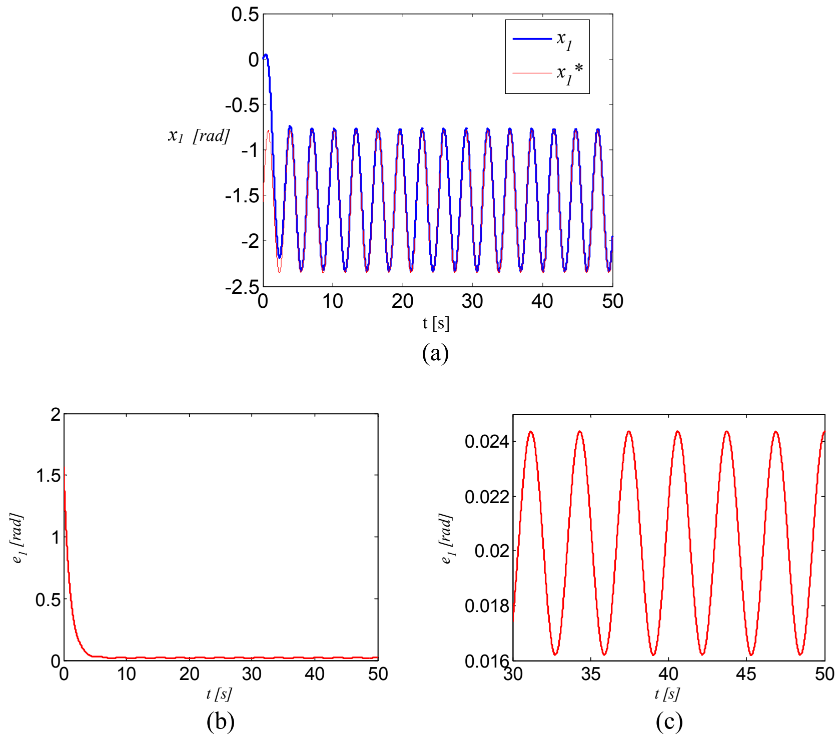

Figure 5. (a) Linear system (18) with control **U** (23). (b) Linear error variation. (c) Error in continuous operation.

Considering the introduction of control (20) obtained from the linearized system (18) in the nonlinear system (12) the following behavior can be obtained, represented by:

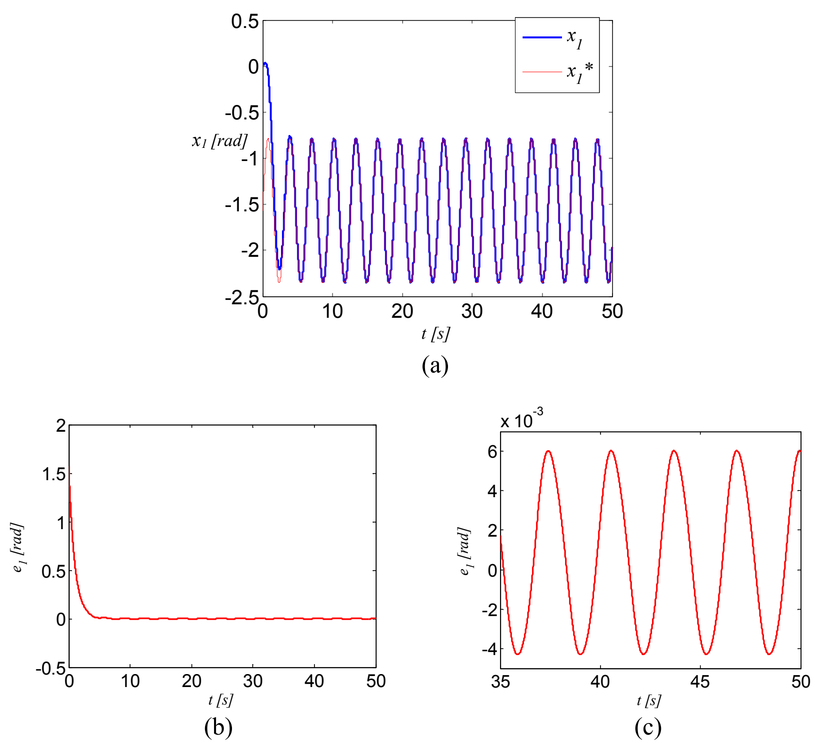

Figure 6. (a) Nonlinear system (12) with control **U** (23). (b) Nonlinear error variation. (c) Error in continuous operation.

As can be verified in Fig. 6 the optimal control strategy obtained for the linear system (18) is also effective for the nonlinear system (12) and the error committed by the proposed control (23) can be obtained.

4. CONCLUSION

As it can be seen, the error committed in the case of the nonlinear system was lower than that obtained for the linear system. As demonstrated by Tusset and Rafikov (2002), with the control strategy using linearized models in this study made it possible to obtain adequate control for nonlinear systems via linearized models.

It was verified that the application of a connecting-rod crankshaft mechanism such as a engine using compressed air energy provides great solutions for application in environments where the electrical installations are difficult to move and/or can create explosion hazards, such as in mining processes.

5. REFERENCES

Ahmad, F. Hitam, A. L., Hudha, K. and Jamaluddin, H., 2011. “Position tracking of slider crank mechanism using PID controller optimized by Ziegler Nichol’s method”. *Journal of Mechanical Engineering and Technology*, Vol. 3. p.27-41.

Awrejcewicz, J. and Kudra, G., 2003. “Modeling na numerical investigation of nonlinear dynamics of a mono-cylinder combustion engine”. In *Proceedings of DETC’03 ASME 2003 Design Engineering Technical Conferences and Computers and Information in Engineering Conference.* Chicago, Illinois, USA.

Boyle, C., Howell, L. L., Magleby, S. P. and Evans, M. S., 2003. “Dynamic modeling of compliant constant-force compression mechanisms”. *Mechanism and Machine Theory*, Vol. 38, p. 1469-1487.

Benhammouda, B. and Vazquez-Leal, H., 2015. “Analytical Solution of a Nonlinear Index-Three DAEs System Modelling a Slider-Crank Mechanism”. *Discrete Dynamics in Nature and Society*, Vol. 2015, p. 1-14.

Chuang, C. W., Lee, C. D. and Huang. C. L., 2006. “Applying Experienced Self-Tuning PID Control to Position Control of Slider Crank Mechanisms”. In *SPEEDAM 2006 International Symposium on Power Electronics, Electrical Drives, Automation and Motion*. IEEE. S21 – 18, S21 – 23.

Chuang, C. W., 2007. “PC-based pseudo-model following discrete integral variable structure control of positions in slider-crank mechanisms”. *Journal of Sound and Vibration*, Vol., p. 510–520.

Fung, R. F., Chiang, C. L. and Chen, S. J., 2009. “Dynamic modelling of an intermittent slider–crank mechanism”. *Applied Mathematical Modelling*, Vol. 33 (2009) 2411–2420.

Ha, J. L., Fung, R. F., Chen, K. Y. and Hsien, S. C., 2006. “Dynamic modeling and identification of a slider-crank mechanism”. *Journal of Sound and Vibration*, Vol. 289, p. 1019–1044.

Kao, C. C., Chuang, C. W. and Fung, R. F., 2006. ”The self-tuning PID control in a slider–crank mechanism system by applying particle swarm optimization approach”. *Mechatronics*, Vol. 16, p. 513–522.

Karkoub, M. A., 2000.”Control of the elastodynamic vibrations of a ¯exible slider±crank mechanism using msynthesis”. *Mechatronics*, Vol. 10, p. 649-668.

Komaita, Y. and Furuta, K., 2008. “Energy Control of Slider-Crank Mechanism”. In *SICE Annual Conference 2008*. The University Electro-Communications, Japan.

Lin, F.J., Fung, R.F., Lin, H.H. and Hong, C. M., 2001. “A supervisory fuzzy neural network controller for slider-crank mechanism”. *Mechatronics*, Vol. 11, p. 227-250.

Liniecki, A., 1970. “Synthesis of a slider-crank mechanism with consideration of dynamic effects”. *Journal of Mechanisms.* Vol. 5, p. 337-349.

Pandian, S. R., Hayakawa, Y., Kanazawa, Y., Kamoyama, Y. and Kawamura S., 1997. “Practical design of a sliding mode controller for pneumatic actuators”. *Journal of Dynamic Systems, Measurement, and Control*, Vol. 119 p. 666–674.

Pedroso, M. D., Nascimento, C. B., Tusset, A. M. and Kaster, M. S., 2013. “A Hyperbolic Tangent Adaptive PID + LQR Control Applied to a Step-Down Converter Using Poles Placement Design Implemented in FPGA”. *Mathematical Problems in Engineering (Print)*, v. 2013, p. 1-8.

Tusset, A. M. and Rafikov, M., 2004. “Controle ótimo de Pragas: Modelos Linearizados, Funcional Quadrático”. *TEMA - Tendências em Matemática Aplicada e Computacional*, Vol. 5, p. 145-154.

Tusset, A. M., Bueno, A. M., Nascimento, C. B., Kaster, M. S. and Balthazar, J. M., 2013. “Nonlinear state estimation and control for chaos suppression in MEMS resonator”. *Shock and Vibration*, Vol. 20, p. 749-761.

Wauer, J. and Bührle, P., 1997. “Dynamics of a Flexible Slider-Crank Mechanism Driven by a Non-Ideal Source of Energy”. *Nonlinear Dynamics,* Vol. 13, p. 221-242.

6. RESPONSIBILITY NOTICE

The authors are the only responsible for the printed material included in this paper.